DOI: 10.1002/cmdc.200800193

Determination of the Critical Amino Acids Involved in the Peroxisome Proliferator-Activated Receptor (PPAR) δ Selectivity of Phenylpropanoic Acid-Derived Agonists

Jun-ichi Kasuga,[a] Takuji Oyama,[b] Izumi Nakagome,[c] Makoto Makishima,[d] Shuichi Hirono,[c] Kosuke Morikawa,[b] Yuichi Hashimoto,[a] and Hiroyuki Miyachi*[a]

The nuclear receptors (NRs) form a superfamily of ligand-dependent transcription factors that control diverse aspects of numerous biological processes and systems including reproduction, development, homeostasis, and immune function. This superfamily includes the steroid and thyroid hormone receptors, the retinoid and vitamin D receptors, as well as a large number of orphan receptors. The structures of NRs are composed of several functionally important regions (designated A to F). The N-terminal A/B region contains a transcriptional activation function-1 (AF-1) motif that works independent of ligand binding. The central DNA-binding region (C) is highly conserved among the NRs and contains two zinc finger motifs that make contact with specific nucleotide sequences, termed hormone response elements. The C-terminal regions (D, E and F) are required for ligand binding and receptor dimerization. In most receptors, this region also contains a second highly conserved transcriptional activation function-2 (AF-2) motif, which is important for ligand-dependent transcription.

Based on the elucidated human genome sequence, 48 NRs are speculated to exist in humans.[1] However, ligands have been identified for only 20–25 of them. The others are so-called orphan receptors, whose endogenous ligands are not yet known.[2,3] Among the NRs, much attention has been focused on the peroxisome proliferator-activated receptors (PPARs) over the past two decades.

PPARs are activated by endogenous saturated and unsaturated fatty acids and their metabolites and synthetic ligands.[4] Three subtypes have been isolated to date, PPARα, PPARδ and PPARγ, which are differentially expressed in a tissue-specific manner. PPARα is predominantly expressed in tissues involved in lipid oxidation, such as liver, kidney, skeletal muscle, cardiac muscle and adrenal gland. PPARγ is expressed in adipose tissue, macrophages and vascular smooth muscle. In contrast to the specific distributions of PPARα and PPARγ, PPARδ is ubiquitously expressed.[5]

Upon ligand binding, a PPAR dimerizes with a nuclear receptor partner, retinoid X receptor (RXR), and the heterodimer regulates gene expression by binding to specific consensus DNA sequences called peroxisome proliferator responsive elements. These elements are a direct repeat of the hexameric AGGTCA recognition motif, separated by one nucleotide (DR1), present in the promoter region of the target gene.[6]

The glitazone-derived antidiabetic agents, such as pioglitazone and rosiglitazone, and fibrate-derived antidyslipidemic agents, such as fenofibrate and bezafibrate, are known ligands of PPARγ and PPARα, respectively. Consequently, research interest has been focused on these two metabolic NR subtypes as therapeutic targets for the treatment of type II diabetes and dyslipidemia. In contrast, research interest in PPARδ has been limited, perhaps because of its ubiquitous distribution. However, the availability of PPARδ knockout animals and selective ligands, in particular GW-501516 (**1**) developed by GlaxoSmith-

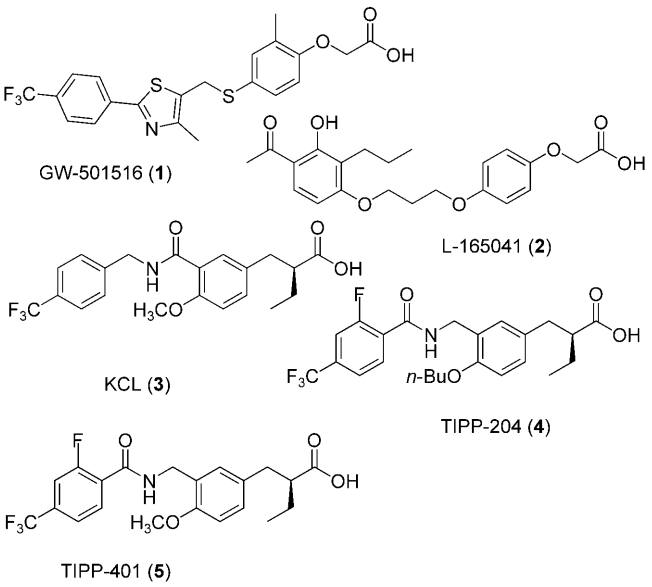

Kline (GSK) and L-165041 (**2**), prompted us to examine the involvement of PPARδ in fatty acid metabolism, insulin resistance, reverse cholesterol transport, inflammation, and other related processes.[7] Recent results from phase I/II clinical studies of GW-501516 demonstrated that a PPARδ agonist elevated HDL cholesterol levels (phase I) and decreased triglyceride (phase I, phase I/II), total cholesterol (phase I/II), and apoB100

[a] J. Kasuga, Prof. Dr. Y. Hashimoto, Prof. Dr. H. Miyachi
Institute of Molecular and Cellular Biosciences, University of Tokyo
Yayoi, Bunkyo-ku, Tokyo 113-0032 (Japan)
Fax: (+81) 3-5841-8495
E-mail: miyachi@iam.u-tokyo.ac.jp

[b] Dr. T. Oyama, Prof. Dr. K. Morikawa
The Takara-Bio Endowed Division
Institute for Protein Research, Osaka University
6-2-3, Furuedai, Suita, Osaka 565-0874 (Japan)

[c] Prof. Dr. I. Nakagome, Prof. Dr. S. Hirono
School of Pharmaceutical Sciences, Kitasato University
5-9-1 Shirokane, Minato-ku, Tokyo 108-8641 (Japan)

[d] Prof. Dr. M. Makishima
School of Medicine, Nihon University
30-1 Oyaguchi-kamicho, Itabashi-ku, Tokyo 173-8610 (Japan)

levels (phase I/II).[8] These observations suggest that PPARδ may be an effective target for the treatment of metabolic syndrome.

Several PPARδ-selective agonists have been reported in the literature, though most are derivatives of GW-501516, i.e., (2-methyl)phenoxyacetic acid derivatives.[9–14] Using KCL (**3**), a hPPARα-selective agonist with the 2-methoxybenzamide moiety, as a lead,[15–19] we designed and synthesized a series of substituted phenylpropanoic acid derivatives as hPPAR agonists. As part of our continuing research on the structural development of subtype-selective PPAR agonists, we designed and synthesized a novel hPPARδ-selective agonist, TIPP-204 (**4**).[20] TIPP-204 exhibited potent hPPARδ transactivation activity and high hPPARδ selectivity. In our assay system TIPP-204 exhibited transactivation activities (EC_{50}) in hPPARδ, hPPARα and hPPARγ of 0.7, 240 and 1400 nM, respectively.

TIPP-204 is structurally distinct from other classes of PPARδ-selective agonist, such as GW-501516, and therefore, we were interested in the reason for its hPPARδ selectivity. Structurally, TIPP-204 differs from the dual hPPARα/δ agonist TIPP-401 (**5**),[21] in the length of the alkoxy group located at the 4-position of the phenyl linker. Therefore, we speculated that the shape of the binding pocket hosting these alkoxy groups may be the critical determinant of hPPARδ-selectivity.

In order to understand the hPPARδ selectivity of TIPP-204, molecular modeling studies were conducted, docking TIPP-401 with the hPPARδ and hPPARα ligand binding domains (LBDs). The binding poses of TIPP-401 with hPPARδ LBD and hPPARα LBD are shown in Figure 1, further details of the molecular modeling studies will be reported in due course. From the results, it was apparent that the methyl portion of the methoxy group of TIPP-401 was buried in a binding cavity of the hPPARδ LBD composed of three amino acids, Val 298 in the β-sheet-2, Leu 303 in the β-sheet-3, and Ile 328 in the helix-7 (RXR LBD crystal structure numbering system[22]). In the case of hPPARα, the corresponding binding cavity hosting the methyl portion of the methoxy group of TIPP-401 is composed of Met 325 in the β-sheet-2 , Met 330 in the β-sheet-3, and Met 355 in the helix-7. The methylthioethyl side chain of Met is bulkier than those of Val, Leu, and Ile, and the cavity volume

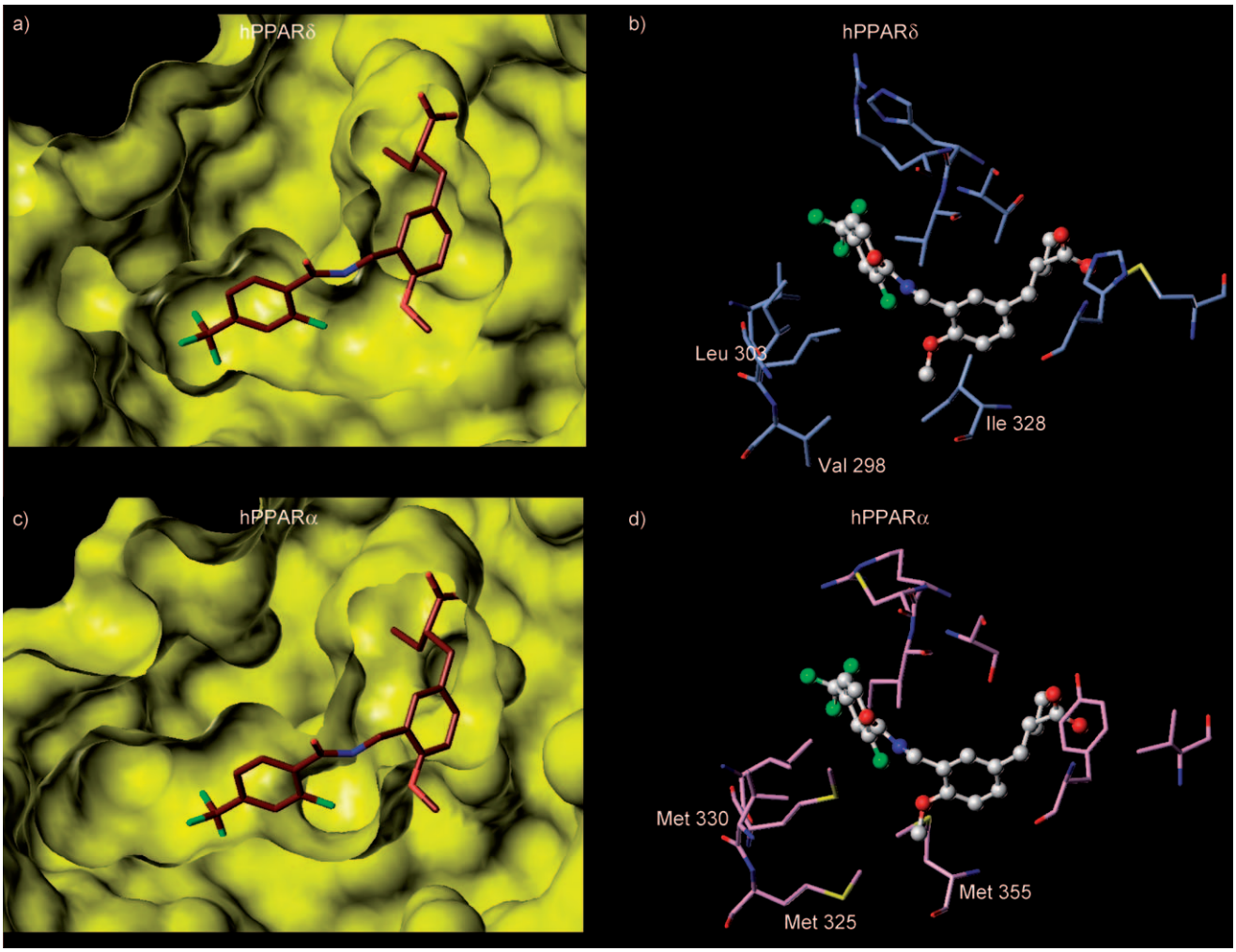

Figure 1. Molecular modeling results of TIPP-401 docked to the LBD of hPPARδ and hPPARα. a) A Connolly's molecular surface map showing the binding pose of TIPP-401 complexed with hPPARδ; b) Key amino acids of the hPPARδ LBD interacting with TIPP-401; c) A Connolly's molecular surface map showing the binding pose of TIPP-401 complexed with hPPARα; d) Key amino acids of the hPPARα LBD interacting with TIPP-401.

of hPPARδ was calculated to be threefold greater than the corresponding hPPARα cavity. Previously we reported that the optimal length of the alkoxyl group of compounds in the TIPP series differs between hPPARα and hPPARδ. A short-chain alkoxy group, such as methoxy or ethoxy, is preferable for potent hPPARα transactivation activity, while a medium-chain alkoxy group, such as *n*-propoxy or *n*-butoxy, is preferable for potent hPPARδ transactivation activity.[20] The differences in activities are consistent with the idea that the alkoxy group interacts with cavities of different volumes in the two hPPARs, and support the validity of the calculated binding configurations.

These binding models are essentially snapshots of the interactions between TIPP-401 and the hPPARs, and while they are adequate to identify the key amino acids for hPPARδ, they were not appropriate to investigate in detail the contributions of the three identified amino acids to the binding of TIPP-204 to hPPARδ. For this purpose, we constructed a set of 6 GAL4-fusion mutant hPPARs (Figure 2 a); i.e., Val 298 of hPPARd was changed to Met (hPPARdV298M), and the corresponding Met of hPPARa was changed to Val (hPPARaM325V), Leu 303 of hPPARd was changed to Met (hPPARdL303M) and the corresponding Met of hPPARa was changed to Leu (hPPARaM330L), and Ile 328 of hPPARd was changed to Met (hPPARdI328M) and the corresponding Met of hPPARa was changed to Ile (hPPARaM355I). As summarized in Figure 2 b, the reporter assays showed that the transactivation activity of TIPP-204 on hPPARδ was retained in the case of the Leu 303M mutant, decreased to some extent in the case of the Ile 328M mutant, but greatly decreased in the case of the Val 298M mutant (~30 times less potent). These three mutations all decrease the size of the cavity hosting the *n*-butoxy group of TIPP-204, and the rank order of the resultant effect on the transactivation activity was Val 298 > Ile 328 ≫ Leu 303. Conversely, the transactivation activities of GW-501516 on the mutant receptors showed that the most important amino acid was different from that observed for TIPP-204. The transactivation activity of GW-501516 on hPPARδ was retained in the Val 298M and Leu 303M mutants, but greatly decreased in the case of the Ile 328M mutant (~20 times less potent). Therefore, unlike TIPP-204, Val 298 is less important than Ile 328 for the hPPARδ selectivity of GW-501516.

As for hPPARα transactivation activity, the replacement of Met 325 with Val greatly increased the activity of TIPP-204,

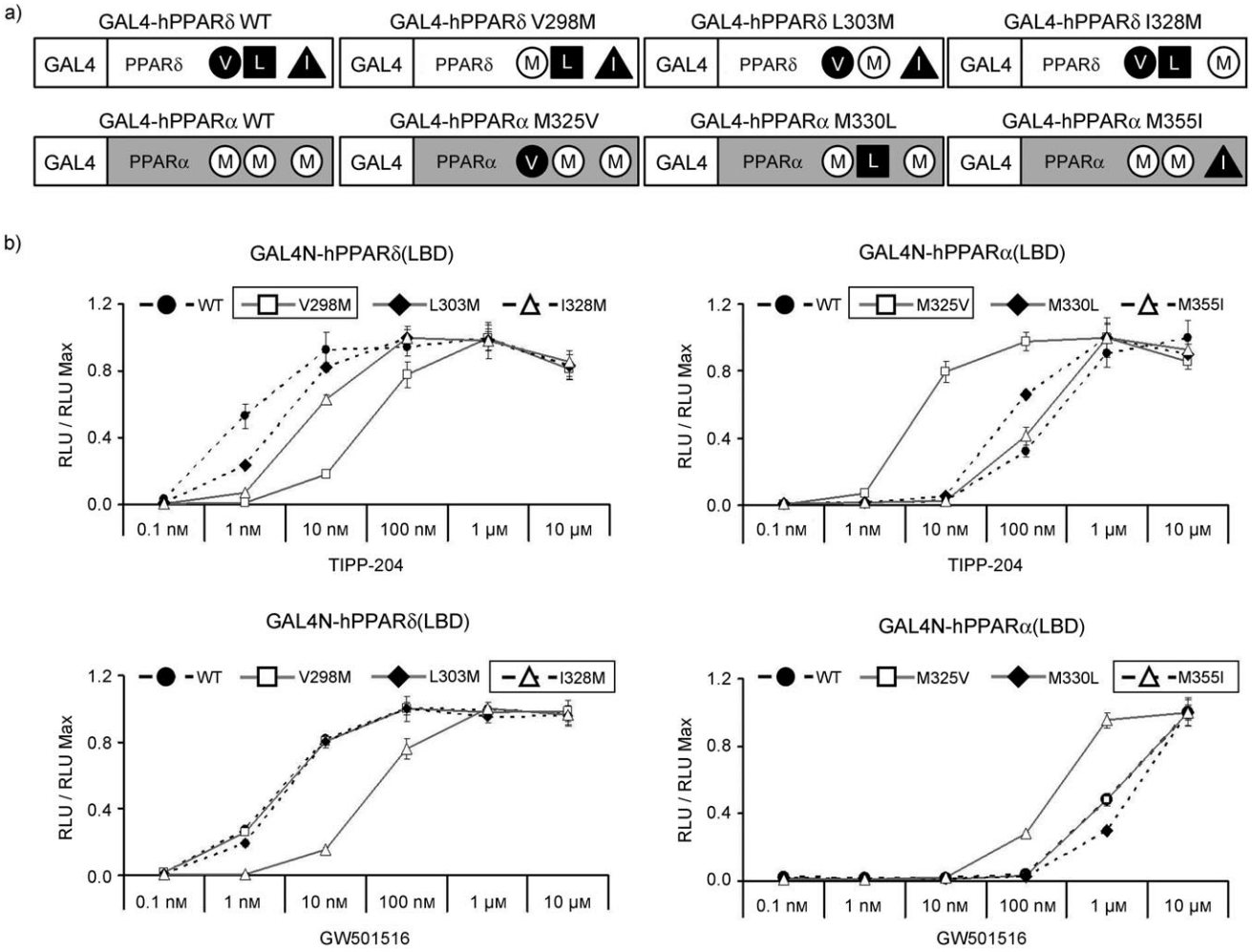

Figure 2. a) A schematic representation of GAL4-fusion point mutants; b) The dose responses for the transactivation of the GAL4-fusion point mutant constructs with TIPP-204 and GW-501516.

while the other mutations had little effect. Conversely, the substitution of Met 355 with Ile, increased the agonist affect of GW-501516, which is a weak agonist of wild type hPPARα. On the contrary, the substitution of Met 325 to Val had no relevant effects.

These mutation studies clearly indicated that the hPPARδ selectivity of TIPP-204 can be largely attributed to favourable interactions between the *n*-butoxy group of TIPP-204 and Val 298 (and to a lesser extent Ile 328) of hPPARδ. Whereas, Ile 328 appears to be the primary determinant of the PPARδ selectivity of GW-501516, and the critical determinant of the PPARα activity of GW-501516 is the corresponding Met 355 of hPPARα.

In order to understand in detail why Val 298 is important for TIPP-204, we solved the X-ray crystal structure of TIPP-204 complexed with the hPPARδ LBD at 3.0 Å resolution (Figure 3). Most of the hPPARδ LBD amino acids were defined in the electron-density map, except for the loop between helix-2′ and helix-3, which is the most thermally mobile loop. The hydrophobic tail of the 2-fluoro-4-(trifluoromethyl)phenyl group is positioned in the pocket formed by helix-2′, helix-3, helix-6, and the β-sheets, as predicted by the modeling studies. The TIPP-204 carboxylate group forms H-bond networks with Thr 253 in helix-3, His 287 in helix-5, His 413 in helix-10, and Tyr 437 in the AF2-helix. Notably, the *n*-butoxy group of TIPP-204 is positioned in the small cavity formed by Val 298 in β-sheet-2, Leu 303 in β-sheet-3, and Ile 328 in helix-7. Val 298 forms the floor, and Leu 303 and Ile 328 form the sides of the cavity (Figure 3 b), giving the shortest distance between Val 298 and the distal methyl group of TIPP-204. This may be the reason why in the Val 298M mutation, elongating the amino acid side chain causes a dramatic decrease in transactivation activity. The distance between Leu 303 and the CH_2 of the *n*-butoxy group in TIPP-204 is somewhat longer than that between Val 298 and the distal CH_3 of the *n*-butoxy group in TIPP-204, so the effect of the Leu 303M mutation is smaller than the Val 298M mutation. The distance between Ile 328 and the CH_2 of the *n*-butoxy group in TIPP-204 is the longest of the three amino acids, and additionally, the distal end of the Ile 328 side chain faces away from the *n*-butoxy group of TIPP-204, which may be the reason why the Ile 328M mutation had little affect the activity.

In summary, we have established that Val 298 is the key amino acid determining the hPPARδ selectivity of the phenylpropanoic acid-derived agonist TIPP-204, while Ile 328 is the key amino acid determining the hPPARδ transactivation activity of the structurally different PPARδ-selective agonist GW-501516. These findings are expected to be helpful for the logical design of new potent hPPARδ-selective agonists.

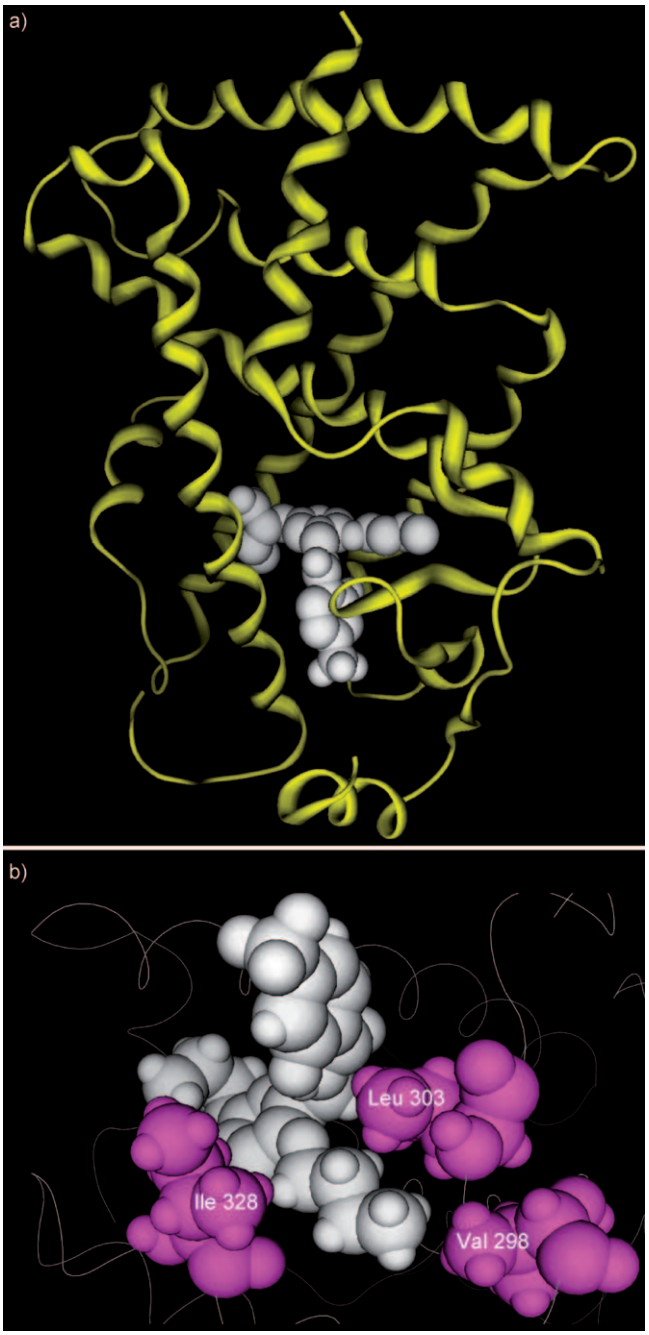

Figure 3. a) An overview of the structure of TIPP-204–hPPARδ LBD complex; b) Close-up view of the *n*-butoxy chain of TIPP-204 in the binding site.

Experimental Section

Chemistry

TIPP-204 was synthesized according to the previously reported method.[20] GW-501516 was purchased from Alexis Biochemicals (Lausen, Switzerland).

Virtual docking: Twenty random conformers of TIPP-401 were generated as input structures with the computer ligand docking program Glide 4.0, to avoid dependence of the docking process on the initial structure. Each conformer was docked into representative 3D-structures of the hPPARδ LBDs (PDB code 1GWX:A, 1GWX:B, 1Y0S:A, 2B50A, and 2J14A) using Glide 4.0 sp mode. The Glide score,[22] which represents the sum of the atomic level ligand–receptor interactions, was calculated for each generated pose. The pose with the best Glide score was selected as the binding pose of TIPP-401 to the hPPARδ LBD. The structure of TIPP-401–hPPARδ LBD complex was superposed on the 3D-structure of hPPARα LBD, the hPPARδ LBD was deleted from the superposed

structures to generate the TIPP-401–hPPARα LBD complex 3D-structure.

Biology

Mutagenesis: All compounds were dissolved in DMSO to give a final concentration of 0.1% in all assays. The GAL4 fusions of the hPPARα LBD and hPPARδ LBD mutants were prepared using a QuikChange site-directed mutagenesis kit (Stratagene, La Jolla, CA, USA). The expression vectors pCMX-GAL4N-hPPARα and pCMX-GAL4N-hPPARδ were used as templates. The presence of the desired mutation was confirmed by DNA sequencing. Primer sequences used for the site-directed mutagenesis were as follows:

hPPARα-M325V: GCTGTCTTCTGTGGTGAACAAAGACGGGATGC (forward) and GCATCCCGTCTTTGTTCACCACAGAAGACAGC (reverse). hPPARα-M330L: GAACAAAGACGGGCTGCTGGTAGCGTATGG (forward) and CCATACGCTACCAGCAGCCCGTCTTTGTTC (reverse). hPPARα-M355I: CCGTTCTGTGATATCATCGAACCCAAGTTTGATTTTGCC (forward) and GGCAAAATCAAACTTGGGTTCGATGATATCACAGAACGG (reverse). hPPARδ-V298M: GCCATGCTGGCCTCTATCATGAACAAGGACGGGC (forward) and GCCCGTCCTTGTTCATGATAGAGGCCAGCATGGC (reverse). hPPARδ-L303M: CAAGGACGGGATGCTGGTAGCCAACGGC (forward) and GCCGTTGGCTACCAGCATCCCGTCCTTG (reverse). hPPARδ-I328M: CGCAAACCCTTCAGTGATATCATGGAGCCTAAGTTTG (forward) and CAAACTTAGGCTCCATGATATCACTGAAGGGTTTGCG (reverse).

Cell Culture and Transactivation Assays: Human embryonic kidney HEK293 cells were cultured in DMEM containing 5% fetal bovine serum and antibiotic–antimycotic (Nacalai, Kyoto, Japan) at 37 °C in a humidified atmosphere of 5% CO_2 in air. Transfections were performed by calcium phosphate co-precipitation. Cells were treated with the ligands eight hours after transfection. Cells were harvested ~16–20 h after treatment, and luciferase and β-galactosidase activities were assayed using a luminometer and a microplate reader. DNA co-transfection experiments included 50 ng of reporter plasmid, 20 ng of pCMX-β-galactosidase, 15 ng of each receptor expression plasmid, and pGEM carrier DNA to make a total of 150 ng of DNA per well in a 96-well plate. Luciferase data were normalized to an internal β-galactosidase control, and reported values are the means of triplicate assays.

X-ray crystallography

The procedures for determining the TIPP-204–hPPARδ co-crystal structure, including the protein purification, crystal growth and structure refinements were as described previously, with some modifications.[24] The atomic coordinates have been deposited in the Protein Data Bank (PDB code 2ZNP). Details of the structural determination of the TIPP-204–hPPARδ co-crystal structure and a series of the hPPAR LBD ligand complex structures will be published in due course.

Acknowledgements

This work was partially supported by Grants-in-Aid for Scientific Research from The Ministry of Education, Culture, Sports, Science and Technology, Japan, and the Japanese Society for the Promotion of Science. T.O. and K.M. wish to thank JSPS Grant-in-aid for Creative Scientific Research Grant 18GS031.

Keywords: receptors · mutagenesis · PPARδ-selective agonists · protein structures · X-ray crystallography

[1] A. Chawla, J. J. Pepa, R. M. Evans, D. J. Mangelsdorf, *Science* **2001**, *294*, 1866.
[2] N. J. McKenna, R. B. Lanz, B. W. O'Malley, *Endocr. Rev.* **1999**, *20*, 321.
[3] V. Giguere, *Endocr. Rev.* **1999**, *20*, 689.
[4] C. D. Banner, M. Göttlicher, E. Widmark, J. Sjövall, J. J. Rafter, J. A. Gustafsson, *J. Lipid Res.* **1993**, *34*, 1583.
[5] T. M. Willson, P. J. Brown, D. D. Sternbach, *J. Med. Chem.* **2000**, *43*, 527.
[6] H. Keller, C. Dreyer, J. Medin, A. Mahfoudi, K. Ozato, W. Wahli, *Proc. Natl. Acad. Sci. USA* **1993**, *90*, 2160.
[7] H. Lim, R. A. Gupta, W. G. Ma, B. C. Paria, D. E. Moller, J. D. Morrow, R. N. DuBois, J. M. Trzaskos, S. K. Dey, *Genes Dev.* **1999**, *13*, 1561.
[8] D. L. Sprecher, A. Johnson, G. Pearce, G. Watts, H. Barrett, *Circulation* **2005**, *112*, (suppl. Abs), 1211.
[9] M. L. Sznaidman, C. D. Haffner, P. R. Maloney, A. Fivush, E. Chao, D. Goreham, M. L. Sierra, C. LeGrumelec, H. E. Xu, V. G. Montana, M. H. Lambert, T. M. Willson, W. R. Oliver, Jr., D. D. Sternbach, *Bioorg. Med. Chem. Lett.* **2003**, *13*, 1517.
[10] C. E. Basséne, F. Suzenet, N. Hennuyer, B. Staels, D.-H. Caignard, C. Dacquet, P. Renard, G. Guillaumet, *Bioorg. Med. Chem. Lett.* **2006**, *16*, 4528.
[11] S. Weigand, H. Bischoff, E. Dittrich-Wengenroth, H. Heckroth, D. Lang, A. Vaupel, M. Woltering, *Bioorg. Med. Chem. Lett.* **2005**, *15*, 4619.
[12] R. Epple, M. Azimioara, R. Russo, B. Bursulaya, S. S. Tian, A. Gerken, M. Iskandar, *Bioorg. Med. Chem. Lett.* **2006**, *16*, 2969.
[13] R. Epple, M. Azimioara, R. Russo, Y. Xie, X. Wang, C. Cow, J. Wityak, D. Karanewsky, B. Bursulaya, A. Kreusch, T. Tuntland, A. Gerken, M. Iskandar, E. Saez, H. M. Seidel, S. S. Tian, *Bioorg. Med. Chem. Lett.* **2006**, *16*, 5488.
[14] R. Epple, M. Azimioara, R. Russo, C. Cow, Y. Xie, X. Wang, J. Wityak, D. Karanewsky, A. Gerken, M. Iskandar, E. Saez, H. M. Seidel, S. S. Tian, *Bioorg. Med. Chem. Lett.* **2006**, *16*, 4376.
[15] M. Nomura, S. Kinoshita, H. Satoh, T. Maeda, K. Murakami, M. Tsunoda, H. Miyachi, K. Awano, *Bioorg. Med. Chem. Lett.* **1999**, *9*, 533.
[16] H. Miyachi, M. Nomura, T. Tanase, Y. Takahashi, T. Ide, M. Tsunoda, K. Murakami, K. Awano, *Bioorg. Med. Chem. Lett.* **2002**, *12*, 77.
[17] H. Miyachi, M. Nomura, T. Tanase, M. Suzuki, K. Murakami, K. Awano, *Bioorg. Med. Chem. Lett.* **2002**, *12*, 333.
[18] M. Nomura, T. Tanase, H. Miyachi, *Bioorg. Med. Chem. Lett.* **2002**, *12*, 2101.
[19] M. Nomura, T. Tanase, T. Ide, M. Tsunoda, M. Suzuki, H. Uchiki, K. Murakami, H. Miyachi, *J. Med. Chem.* **2003**, *46*, 3581.
[20] J. Kasuga, I. Nakagome, A. Aoyama, K. Sako, M. Ishizawa, M. Ogura, M. Makishima, S. Hirono, Y. Hashimoto, H. Miyachi, *Bioorg. Med. Chem.* **2007**, *15*, 5177.
[21] J. Kasuga, Makishima, Y. Hashimoto, H. Miyachi, *Bioorg. Med. Chem. Lett.* **2006**, *16*, 554.
[22] W. Bourguet, M. Ruff, P. Chambon, H. Gronemeyer, D. Moras, *Nature* **1995**, *375*, 377.
[23] T. A. Halgren, R. B. Murphy, R. A. Friesner, H. S. Beard, L. L. Frye, W. T. Pollard, J. L. Banks, *J. Med. Chem.* **2004**, *47*, 1750.
[24] H. Xu, M. Lambert, V. Montana, D. Parks, S. Blanchard, P. Brown, D. Sternbach, J. Lehmann, G. Wisely, T. Willson, *Mol. Cell* **1999**, *3*, 397.

Received: June 27, 2008
Revised: August 1, 2008
Published online on October 16, 2008

